AD-A139 917 TOWARD IN-SITU BUILDING R-VALUE MEASUREMENT(U) COLD REGIONS RESEARCH AND ENGINEERING LAB HANOVER NH S N FLANDERS ET AL. JAN 84 CRREL-84-1 1/1

UNCLASSIFIED F/G 13/2 NL

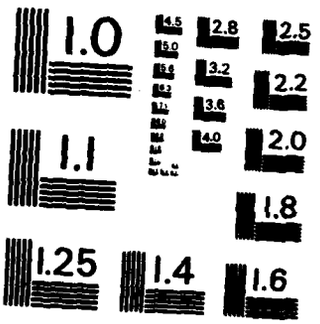

CRREL REPORT 84-1

US Army Corps of Engineers
Cold Regions Research & Engineering Laboratory

Toward in-situ building R-value measurement

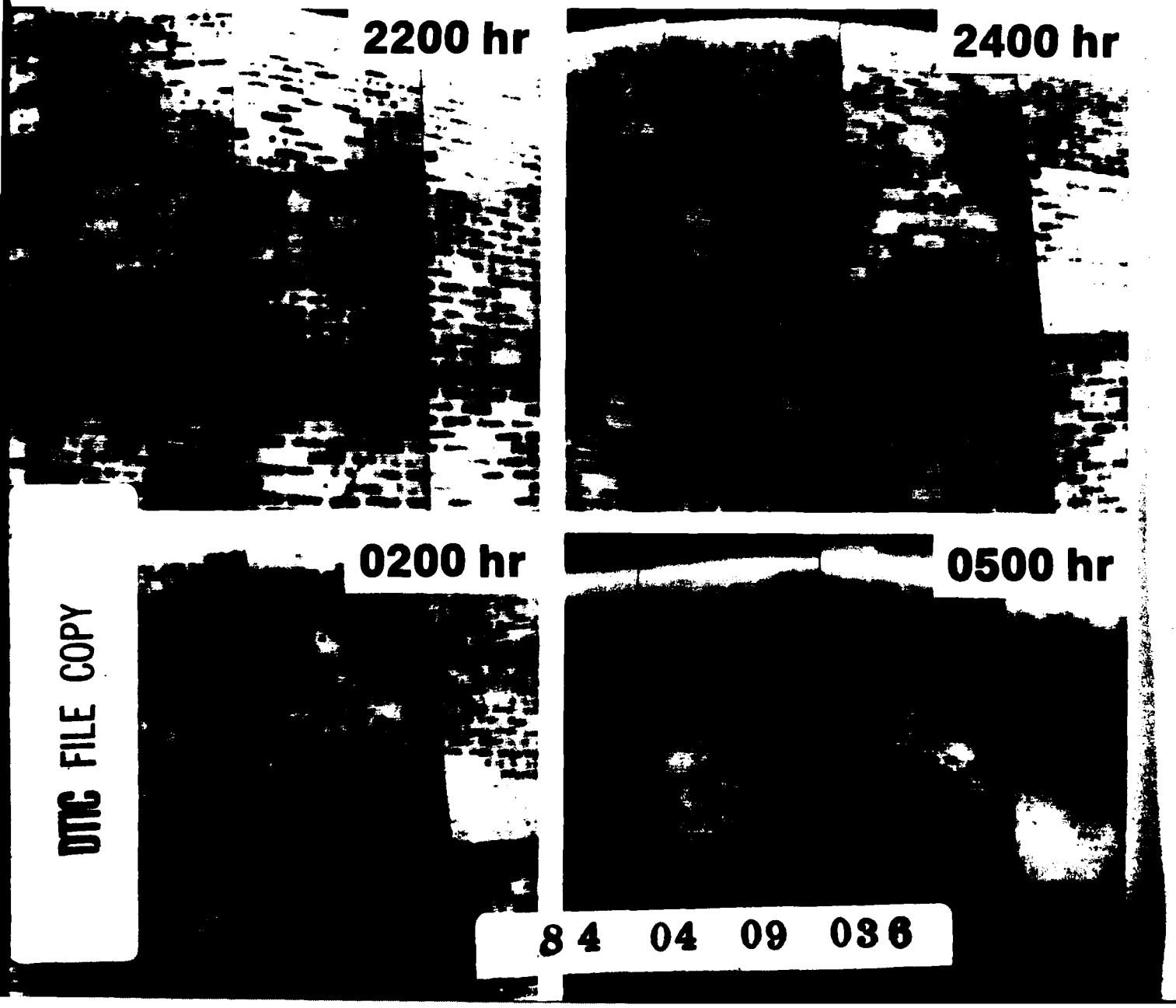

Cover: Composite thermograms of masonry wall studied, at 10 p.m. (top left), midnight (top right), 2 a.m. (bottom left), and 5 a.m. (bottom right). The sequence shows the wall's primary heat transfer modes: at first, giving up stored heat, and later resisting the flow of heat from inside to outside.

CRREL Report 84-1

January 1984

Toward in-situ building R-value measurement

Stephen N. Flanders and Stephen J. Marshall

Prepared for
OFFICE OF THE CHIEF OF ENGINEERS
Approved for public release; distribution unlimited

Unclassified

SECURITY CLASSIFICATION OF THIS PAGE (When Data Entered)

REPORT DOCUMENTATION PAGE		READ INSTRUCTIONS BEFORE COMPLETING FORM
1. REPORT NUMBER CRREL Report 84-1	2. GOVT ACCESSION NO. AD-A139 917	3. RECIPIENT'S CATALOG NUMBER
4. TITLE (and Subtitle) TOWARD IN-SITU BUILDING R-VALUE MEASUREMENT		5. TYPE OF REPORT & PERIOD COVERED 6. PERFORMING ORG. REPORT NUMBER
7. AUTHOR(s) Stephen N. Flanders and Stephen J. Marshall		8. CONTRACT OR GRANT NUMBER(s)
9. PERFORMING ORGANIZATION NAME AND ADDRESS U.S. Army Cold Regions Research and Engineering Laboratory Hanover, New Hampshire 03755		10. PROGRAM ELEMENT, PROJECT, TASK AREA & WORK UNIT NUMBERS DA Project 4A762730AT42, Task C, Work Unit 10
11. CONTROLLING OFFICE NAME AND ADDRESS Office of the Chief of Engineers Washington, D.C. 20314		12. REPORT DATE January 1984 13. NUMBER OF PAGES 20
14. MONITORING AGENCY NAME & ADDRESS(if different from Controlling Office)		15. SECURITY CLASS. (of this report) Unclassified 15a. DECLASSIFICATION/DOWNGRADING SCHEDULE

16. DISTRIBUTION STATEMENT (of this Report)

Approved for public release; distribution unlimited.

17. DISTRIBUTION STATEMENT (of the abstract entered in Block 20, if different from Report)

18. SUPPLEMENTARY NOTES

19. KEY WORDS (Continue on reverse side if necessary and identify by block number)

Buildings	R-values	Thermocouples
Heat flow sensors	Thermal insulation	Thermopiles
Infrared cameras	Thermal measurement, in situ	Walls
Roofs	Thermal resistance	

(delta T)

20. ABSTRACT (Continue on reverse side if necessary and identify by block number)

A technique for measuring the thermal resistance (R-value) of large areas of building envelope is under development. It employs infrared thermography to locate radiant temperature extremes on a building surface and to provide a map of normalized temperature values for interpolation between locations. Contact thermal sensors (thermocouples for temperature and thermopiles for heat flow) are used to calculate the R-value at specific locations by summing the output from each sensor until the ratio between temperature difference (ΔT) from inside to outside surface and heat flow converges to a constant value. R-value measurements of a wood frame insulated wall were within 13% of the expected theoretical value. Similar measurements of a masonry wall were 31 and 43% less than expected. Experimentation

DD FORM 1 JAN 73 1473 EDITION OF 1 NOV 65 IS OBSOLETE

Unclassified

SECURITY CLASSIFICATION OF THIS PAGE (When Data Entered)

20. Abstract (cont'd). delta T

demonstrated that a large ΔT was the single most important variable affecting accuracy and speed of convergence. Thermal guards around heat flow sensors were of little value, according to both experimentation and computer simulation. Attempts to match the absorptivity of sensors with their surroundings may have been insufficient to diminish about 10% of the remaining error in measurement. Lateral heat flow and convection may have been significant problems for accuracy in the masonry construction. Currently, an investigator cannot rely on the literature for guidance in assessing the limitations on accuracy for in-situ building R-value measurement.

PREFACE

This report was written by Stephen N. Flanders, Research Civil Engineer, Civil Engineering Research Branch, Experimental Engineering Division, and Stephen J. Marshall, Physical Science Technician, Research Division, U.S. Army Cold Regions Research and Engineering Laboratory. The study was funded by the U.S. Army Corps of Engineers under DA Project 4A762730AT42, Task C, Work Unit 10, *Improving the Thermal Performance of Military Buildings.*

The report was technically reviewed by Dr. Virgil Lunardini and Dr. Andrew Assur of CRREL. The authors thank Doris Van Pelt and Ronald Domingue for their work in obtaining calibration data for the sensors used in this study.

CONTENTS

ILLUSTRATIONS

Figure

TABLES

Table

TOWARD IN-SITU BUILDING R-VALUE MEASUREMENT

Stephen N. Flanders and Stephen J. Marshall

INTRODUCTION

Measurement of building envelope thermal performance reveals the potential for investment in improved insulation, in both existing and new construction. We are developing a technique for such measurement. It combines localized thermal measurements, using heat flow and temperature sensors, with infrared (IR) thermal mapping to assess the R-values of large areas. In this paper we summarize our efforts to date, which encompass measurements of wood frame and masonry buildings. The technique that we and other investigators have employed is reasonable, but requires further exploration so that all factors affecting accuracy are better controlled.

In brief, an IR scanner first surveys the area to determine the apparent warmest and coolest locations on the building surface. Contact thermal sensors at these locations then provide heat flow and temperature data that determine the areas of highest and lowest thermal resistance (R-value). A thermographic map that depicts all the gradations of temperature between the instrumented locations is prepared, forming the basis for interpolating R-values for each location. We outline this technique in Flanders and Marshall (1981).

The investigation reported here encompassed field measurements of masonry and frame constructions. The masonry construction was a cavity wall of brick and concrete blocks. The wood frame construction incorporated full-thickness insulation between 89-mm-deep 2×4 studs and rafters. Computer simulations of overall wall behavior and of heat flow around the sensors provided an independent check on the field results. Laboratory investigations demonstrated the different effects of sensor configuration and calibration methods.

Other investigators (for example, Treado 1980) have achieved good agreement between measured and calculated values for thermal performance of building envelopes. On the other hand, our work with masonry construction (Flanders and Marshall 1982) resulted in measured R-values that were 57% of those expected for locations containing no insulation. The large discrepancies cast doubt on how well the results reflected the actual performance of masonry construction. Our measurement of four walls and two roof surfaces of a frame building, reported here for the first time, gave us measured R-values only 13% less than the theoretical value. These results suggest difficulties with measuring masonry construction and that the technique may be reasonably accurate for frame construction.

R-VALUE MEASUREMENTS ON A FRAME BUILDING

A 4.2- by 7.3-m frame building with a 12.5° pitched roof was instrumented with heat flow sensors (HFS's) and thermocouples on each of four walls and the two halves of the low-pitch gable roof (see Fig. 1). Simultaneous recording of data from these locations demonstrated the effect of orientation of construction on the measurement (the building axes are rotated 18° clockwise of the true compass axes). Figure 2 shows the typical roof and wall construction, which

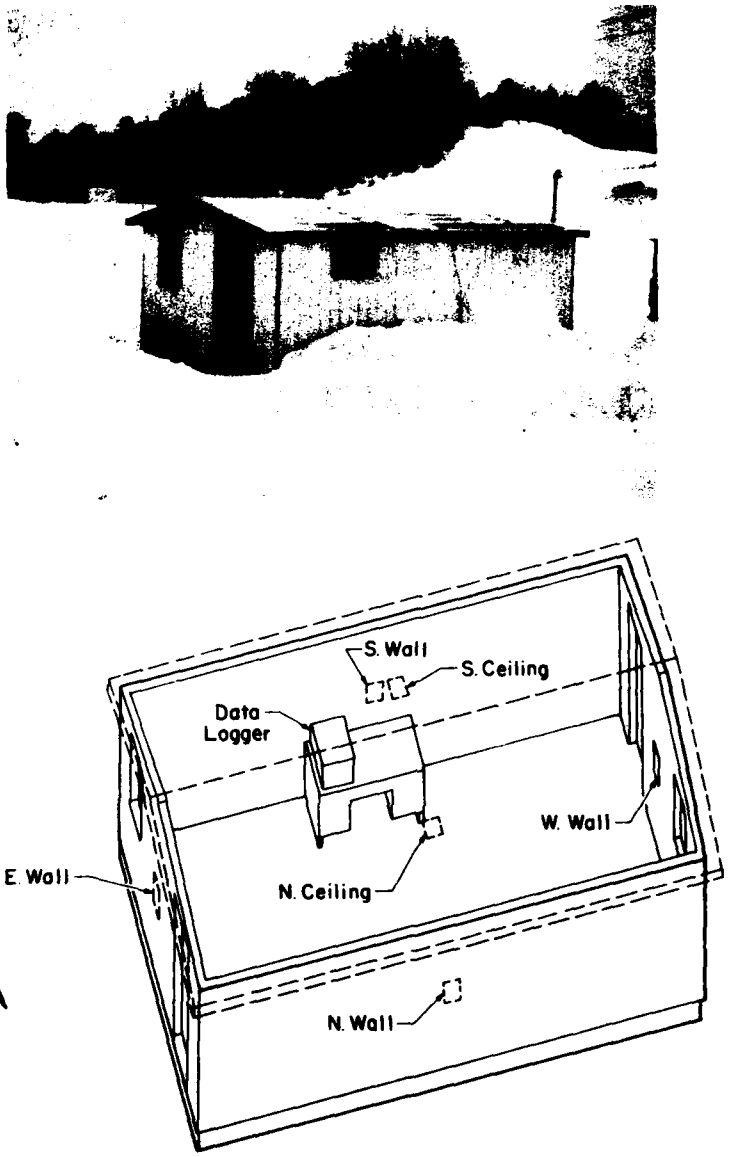

Figure 1. The frame building tested (top). The site is sheltered between two ridges against prevailing winds, which are light. Sensor locations on the building (bottom).

incorporated 89 mm of insulation throughout. Each of the six sensor locations was equidistant between framing members.

Each sensor location employed thermocouples on indoor and outdoor surfaces and an HFS on the indoor surface. Each outdoor wall thermocouple had a 12 by 12 mm gable roof projecting over it for shade against direct sunlight. A strip of vinyl covered the thermocouple on the roof.

We used two types of HFS's, one with and one without a built-in guard surrounding the sensing area. The guarded sensor incorporated a thermopile measurement area of 25 by 13 mm within an overall area of 73 by 111 mm and it was 3.2 mm thick. The material was an unidentified laminated plastic resin. The unguarded sensor had a shiny black-coated layer of aluminum bonded to a dull black plastic sheet containing the thermopile. Its overall dimensions were 13 by 51 by 2.5 mm.

The HFS's were calibrated in a Rapid-k heat flow

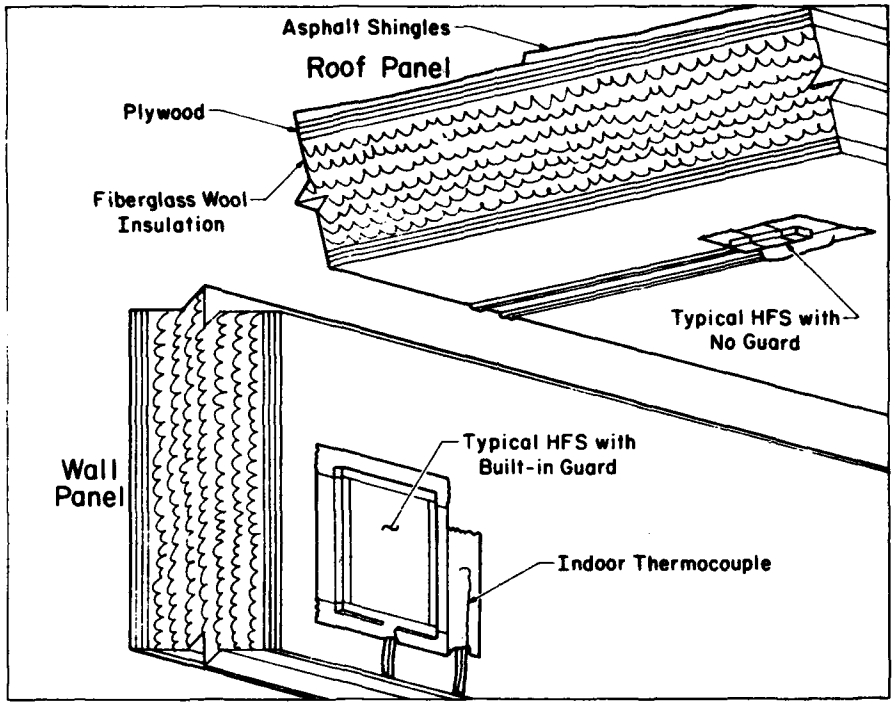

Figure 2. Typical construction of the frame building, incorporating 2×4s spaced 40.6 cm on center in both the roof and wall.

meter thermal conductivity testing machine, which maintains set temperatures on the upper and lower faces of a 0.3-m specimen and reads heat flow from a 100-mm square region in the center. The test specimen had three 0.3-m square layers of material with a total resistance of 0.85 K·m^2/W; the sensor was embedded in the middle layer. The top layer was 6 mm of neoprene foam and the bottom layer 25 mm of rigid fiberglass insulation. Between these was a 3-mm sheet of Micarta (a paper-reinforced phenolic resin) with a cutout in the center to accommodate the HFS. The calibration temperatures were chosen to approximate the temperature that the HFS would function at when in use.

The HFS's were taped to the interior surface with a layer of petroleum jelly between the surface and sensor to provide thermal contact. The tape surrounded the edge of the sensor, overlapping it by about 5 mm. The indoor thermocouple was taped adjacent to the HFS. A sheet of white paper covered the indoor sensors at each location to damp fluctuations in heat flow readings due to convection and to mask the sensor's absorptivity to blend with its surroundings.

A thermographic survey at a ΔT (difference between indoor and outdoor surface t mperature) of about 20°C revealed thermal nalies in the stud bays, despite the presence of surface water stains. In particular, there was no evidence of air leakage or convection in the plane of the construction.

We began recording data on 19 March 1981 at 30-minute intervals and stopped after 750 hours. During this time the outdoor dry bulb temperatures averaged maximums of 13°C each day and minimums of -2.4°C with a 3°C warming trend. The wind averaged over each day 1.5 m/s from the west with a maximum average speed for one day of 3.5 m/s. Twelve days with precipitation were 2.6 days apart on the average.

The R-value was calculated by summing all ΔT data and dividing by the sum of all heat flux data

$$R = \Sigma \Delta T / \Sigma Q \qquad (1)$$

where Q is the heat flux. Equation 1 is the ratio of average values for ΔT and Q which, as the constant terms in a Fourier series of time-variant data, approximate the definition of R under steady-state conditions when the measurement lasts long enough for the equation to converge on a steady value. Both Treado (1980) and Johannesson (1979) advocate the use of eq 1 or its equivalent in integrals derived in Appendix A. Figure 3 shows a typical data plot with the resulting plot of R, according to eq 1.

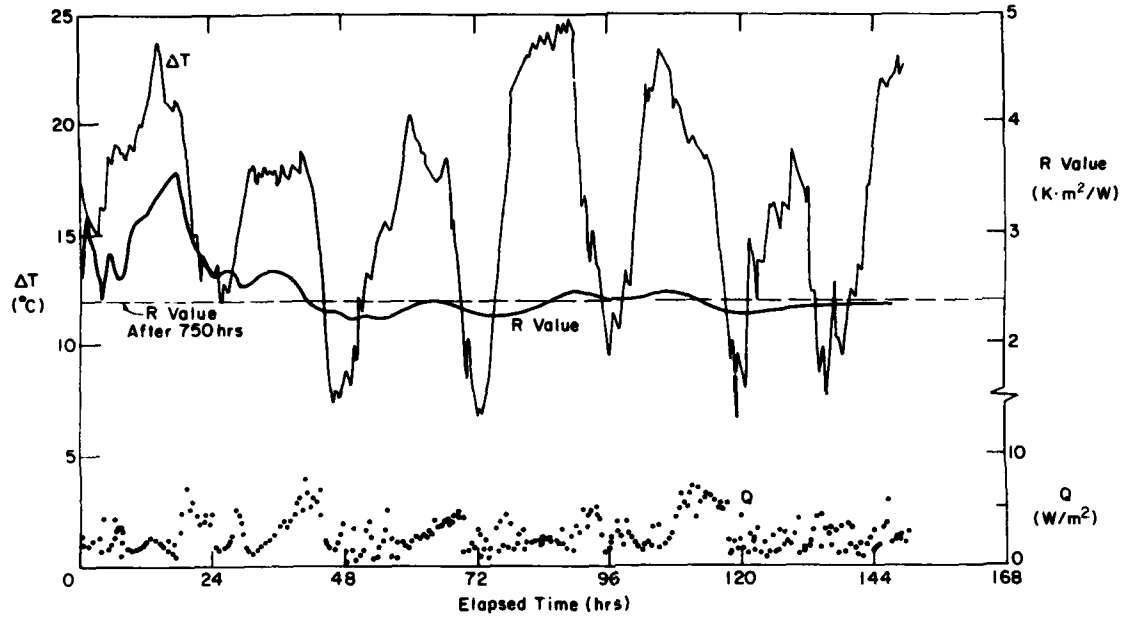

Figure 3. R-value from eq 1. As ΔT and Q accumulate, R-value converges to a constant figure.

Table 1. R-values (K·m²/W) calculated according to eq 1 for 750 hr of data obtained from frame building. Expected R-value = 2.29 K·m²/W for all measurement sites.

	Wall Orientation				*Roof Orientation*	
Measure	*N*	*E*	*S*	*W*	*N*	*S*
R-values	2.1	1.8	2.0	2.0	2.2	1.9
Percent difference from expected	-9	-23	-13	-13	-4	-19

Table 2. Consistency of R-value readings taken in 150-hr blocks expressed as a percentage of the cumulative 750-hr value. Values greater than 100% were more than the 750-hr value.

Period	*Wall Orientation*				*Roof Orientation*	
(hr)	*N*	*E*	*S*	*W*	*N*	*S*
0–150	99	83	99	99	89	84
150–300	103	124	102	106	103	104
300–450	97	99	96	101	108	98
450–600	101	102	100	102	109	106
600–750	99	108	99	97	97	106
Average %	100	103	99	101	101	100
Std. dev. %	2	14	2	3	8	9

Table 1 summarizes the results for walls and roofs with the same expected R-value of 2.29 K·m²/W. All R-values calculated from the data averaged 13% less than the expected value based on the thermal resistances of the constituent materials listed in ASHRAE (1977).

Dividing the data into five groups of readings 150 hr in duration caused about the same percentage difference from the expected value, but the scatter of calculated R-values had a standard deviation that ranged from ± 2 to 11 percentage points around the percent difference shown in Table 1.

The data for each 150-hr block were, on the whole, repeatable. The R-value obtained during any one period for most locations was within a standard deviation of 10% of the long-term 750 hr value, as Table 2 shows.

The deviations of calculated R-values from expected shown in Table 1 probably reflect the accuracy of the measurement, based on our thermography, which detected no air movement at $\Delta T = 26.1°C$, and based on an independent check of the R-value of the frame construction. A 0.3-m square specimen of fiberglass wool insulation was obtained from directly behind the south wall sensor location (Fig. 1). The specimen was placed in a Rapid-k thermal conductivity testing machine. The R-value obtained from this steady-state laboratory test was only 4% less than the value listed in ASHRAE (1977).

Since the plywood skins of the construction constitute such a small portion of the overall thermal resistance, they could not be responsible for the difference between the measured and expected R-values in the field tests. The sensors were located where heat flow should be perpendicular to the plane of the wall. Therefore, we must ascribe the discrepancies to the measurement process. The problem is to identify which factors are important sources of error and how to correct them. Although Table 1 indicates that the measurement technique is somewhat biased, Table 2 demonstrates that the measurements are repeatable.

FACTORS AFFECTING ACCURACY OF MEASUREMENT

There are several possible sources of inaccuracy in the measurement and calculation of R-values, including:

- Insufficient combination of ΔT and measurement duration for a converged calculation, according to eq 1.
- Multidimensional heat flow around the HFS, and lateral heat flow within the construction due to conduction or air movement.
- Inadequate thermal contact of the HFS or thermocouple with the construction.
- Unrepresentative exposure of sensors to sources of infrared radiation.

The effects of time and ΔT

The frame building was measured for more than 750 hr. With an average ΔT of about 11°C, this would give ample time for the proportion of unresolved transient heat flow responses (Q) to varying ΔT inputs that have not resulted in a heat flow response on the indoor surface to be very small. Therefore, we took the cumulative R-values after 750 hr to be the reference values for comparing with the R-values obtained during each 150-hr interval. Not only did the value of R obtained during each interval vary, as mentioned above, but the period necessary for it to stabilize within 10% of the 750-hr value varied, from less than 10 up to 76 hr for walls. Roofs required longer times, as Figure 4 demonstrates.

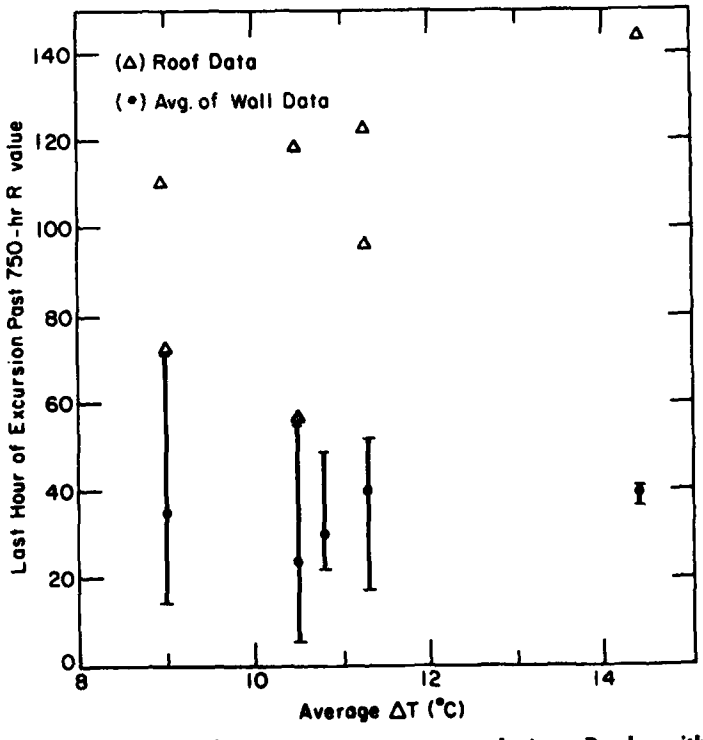

Figure 4. Duration of measurement necessary to obtain an R-value within 10% of the value obtained after 750 hr as a function of averaged ΔT. Each set of data for an average ΔT commences at the beginning of the first of five consecutive 150-hr periods.

Time to stabilize within 15% of the 750-hr R-value was not a strong function of ΔT within the range of ΔT values we observed.

Our work with masonry walls (Flanders and Marshall 1982) encompassed a much wider range of ΔT values and demonstrated that ΔT is the most powerful variable affecting the speed of convergence at an R-value (calculated with eq 1). In that paper we reported that extending the measurement of R for a masonry wall to 473 hr changed the calculated result by only 8% of the value obtained after 116 hr.

Multidimensional heat flow

Multidimensional heat flow around an HFS can result both from the nature of the construction and from how the sensor itself affects the area subject to measurement. The masonry wall we reported on (Flanders and Marshall 1982) had a variety of paths that would keep heat from flowing perpendicularly through the construction (shown in Fig. 5). Masonry ties concentrated the heat flow between the brick and concrete block sides of the construction. Nonetheless, applying the HFS at different places along the face of the concrete block resulted in at most an 8% variation.

The effect of the HFS on the surface being measured must be defined. Schwerdtfeger (1970) illustrates the importance of the comparative thermal conductivities of an HFS and the homogeneous medium surrounding it (he was primarily interested in heat flow through soils). Given the geometry of an HFS, he demonstrated that heat flow through the sensor can be as much as 1.8 or as little as 0.2 that through the surrounding material. This varies as the ratio of the two thermal conductivities, $k_{sensor}/k_{material}$, ranges from 0.1 to 10.

Heat flow through a building surface represents a different situation from Schwerdtfeger's. The HFS shape and conductivity, the conductivity of the building surface, and the effect of air convecting on the back side of the sensor become factors affecting whether heat flow is perpendicular through the surface. To assess this effect, we conducted experiments in a large-scale calibrated hot box and simulated heat flow with a finite-difference computer program.

The calibrated hot box-type thermal testing box consisted of two constant temperature chambers, one refrigerated and the other heated, on either side of a 3.7- by 2.4-m test wall. The wall was made of extruded polystyrene foam, 50.8 mm thick. Four sensors (two guarded and two unguarded HFS's as described earlier) were installed midway up the wall. A 0.3-m square by 3-mm thick Micarta guard had a cutout in the center to accommodate the two sizes of HFS. The thermal resistance of the Micarta and the two types of HFS were unknown, but are believed to be similar. Table 3 demonstrates the effect of the guard.

The net effect of having the guard for either sensor type was a 5% reduction in heat flow through the HFS. Since the heat flow through the sensor

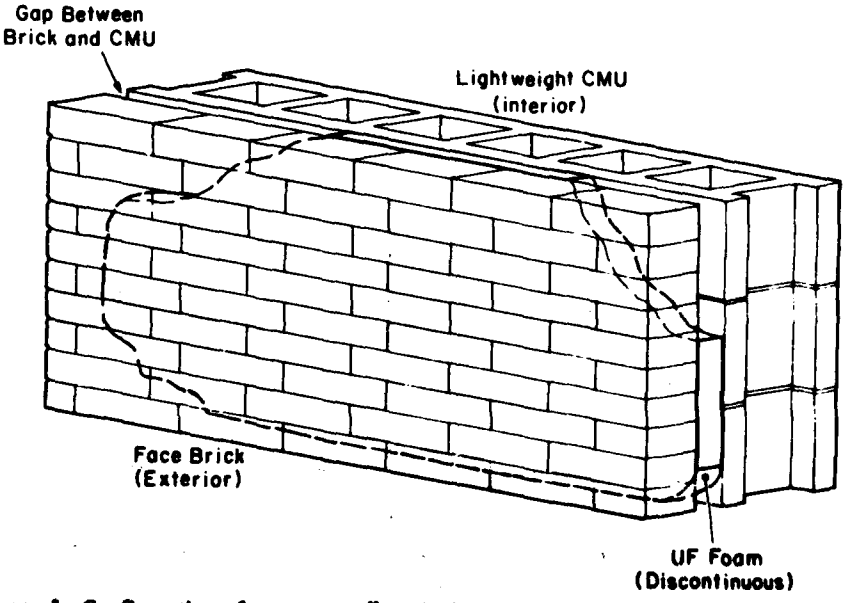

Figure 5. Configuration of masonry wall studied. Webs in concrete blocks and masonry ties divert heat flow from a path perpendicular to the construction.

Table 3. Ratio of heat flow measured with the HFS (Q_{meas}) and that expected from the material properties and dimensions (Q_{exp}); italics denote a reading with a guard.

	Small HFS *Sensor no.*		*Large HFS* *Sensor no.*	
Measure	*1*	*2*	*3*	*4*
Q_{meas}/Q_{exp}	1.10	1.04	*0.94*	1.02
	1.02	1.02	0.99	0.99
	1.10	*0.91*	0.99	0.99
	1.16	0.99	0.97	*0.95*
Average, no guard	1.10	0.98	1.00	1.02
Guard/ave. no guard	0.93	0.97	0.96	0.90

without the guard was very close to that expected, the guard constituted no benefit for that combination of HFS and building material.

Another test was designed to test the extremes to which an HFS might distort the results when the surface material was much more highly conductive than the HFS. This test employed a 0.3-m square specimen consisting of a 6.4-mm thick aluminum plate and a 25.4-mm thick extruded polystyrene board. These were placed in the Rapid-k thermal testing machine without closing the internal platform that normally presses the specimen against the upper and lower surfaces of the test chamber. Instead, an HFS placed on top of the specimen and covered with paper was adjacent to an air space.

With the polystyrene as the top material of the specimen, the HFS affixed to it indicated 9% more heat flow than expected for the test setup. With the aluminum as the top material, two runs gave readings that were 69% higher than expected from the HFS. This test requires further refinement because of the high lateral conduction of the aluminum, but it demonstrates the order of magnitude of discrepancy possible when the HFS monitors a highly conductive material.

To test the extent to which an HFS disturbs heat flow on a wooden surface backed with fiberglass, a computer simulation employed the finite-difference approach to solving the steady-state condition. A grid, consisting of 1.27-mm square nodes, 89 nodes across and 18 nodes thick, simulated half of the long dimension of an HFS in two dimensions. Semi-infinite nodes surrounded two sides of this region. Along the line of symmetry there were flux nodes with no lateral flux. The side with the HFS was represented with convective nodes adjacent to the exposed surfaces of wall and sensor. Nodes at top and bottom of the grid were a constant temperature at a semi-infinite distance away.

The simulation indicated that heat flow at the center of the sensor, which represented the larger of the two sensors we employed, might be 93% of the flow where there was no HFS. A similar analysis with the HFS on a concrete block resulted in a reading of 99% of the undisturbed value.

We concluded that the guard does not contribute a significant benefit for thermal measurements.

Thermal contact and convection

Johannesson (1979) reported that a 1-mm or smaller air gap between the sensor and the building surface has a minimal effect on sensor accuracy. We tested a commercial heat-conductive compound and a petroleum jelly to prevent convection behind the HFS and to improve thermal contact. We also covered the indoor sensors with paper to minimize fluctuations in the readings. Both tests employed the large-scale calibrated hot box described earlier.

The heat-conductive compounds had no significant effect on sensor readings. The HFS readings with petroleum jelly underneath the sensors were 99% of those without the jelly, with a standard deviation of 2%. The commercial compound caused readings 102% of the base case with a standard deviation of 5%.

The combination of paper and petroleum jelly did improve the constancy of the output from the HFS's. Whereas the base case, demonstrated in Table 3, resulted in a standard deviation of 2 to 5% of the heat flux reading, the addition of a paper cover and petroleum jelly between sensor and wall diminished the variability to between 2 and 3.5%, an average reduction of the basic standard deviation by about 27%.

Exposure of sensors to sources of IR radiation

The R-values reported in Table 1 indicate that orientation of the surface with respect to the sun affects the measurement accuracy. The sensors on the north-facing wall and roof gave readings only 6 and 4% less than the theoretical expected value. However, with a 12.5° roof pitch and a 52° average angle between the sun's ecliptic and the horizon, the northerly roof surface received more solar radiation than did the northerly wall. The readings from the other orientations were 12 to 23% less than the expected, although the south-facing surfaces did not necessarily have the greatest variation.

If the outdoor temperature sensors were reading higher than the temperature of the surface to which they were attached, then the ΔT between indoor and

outdoor thermocouples would be less than the ΔT between indoor and outdoor surfaces. This would cause the R-value calculation from eq 1 to be less than the actual value.

The indoor sensors are similarly vulnerable to inaccuracy from absorbing thermal radiation differently than the surface they are supposed to monitor. A nominal solution to this problem is to select a cover that has the same absorptivity as the interior finish of the construction. Since the absorptivity of most materials at near room temperature radiation is about 0.9, a sheet of paper should suffice.

A few cautionary notes, however: the absorptivity of some pastel-colored paints may be as low as 0.3 (Marshall 1981). Likewise, the absorptivity of white paper can range from 0.7 to 0.9. Furthermore, even if the cover does not touch the sensors, some heat from the cover may be transferred to the sensors via radiation, thereby diminishing the value of the cover as a way to eliminate variation in absorptance.

Measurement improvements needed

Probably the most significant source of error in the measurements of the wood-frame construction was the outdoor sensors, which registered higher than representative temperatures. Further work will determine how severe this effect is and how to diminish it.

The exterior sensors also probably contributed to the discrepancies reported in our ASHRAE paper (Flanders and Marshall 1982) on measuring masonry wall thermal conductivity. However, lateral heat flow through the masonry construction may be a bigger cause for error than we surmised. Furthermore, convection within the masonry construction may have worsened its thermal performance more than expected.

CONCLUSION

One reason for addressing the accuracy of thermal measurements is to gain an understanding of the variables that will permit the development of recommended practices for the use of heat flow sensors and thermocouples for characterizing the thermal performance of building envelopes. Currently, an investigator cannot rely on the literature for guidance in assessing the limitations of such thermal measurements or in obtaining a desired level of accuracy.

Such a recommended practice will address the use of sensors, sensor placement, acceptable thermal conditions, and measurement duration, among other considerations. Some of the most important recommendations are listed below.

Sensors

- Calibrate heat flow sensors under conditions that correspond to those of the test; e.g. for a frame wall test, calibration in a vertical orientation with gypsum board on one side and air on the other.
- Mask all sensors with a material of the same absorptivity.

Sensor location

- Avoid known areas of lateral heat flow from conduction and air flow
- Employ thermography, where possible, to identify thermal anomalies.

Thermal conditions

- Identify tradeoffs between ΔT and duration of measurement.

Duration of measurement

- Determine when sufficient data have been obtained.

For now, it is the accuracy, not the repeatability, of the technique that needs improvement.

REFERENCES

ASHRAE (1977) ASHRAE Handbook of Fundamentals. New York, American Society of Heating, Refrigerating and Air Conditioning Engineers.

Flanders, S.N. and S.J. Marshall (1982) In situ measurement of masonry wall thermal resistance. *ASHRAE Transactions.* Vol. 88, Pt. 1. New York: American Society of Heating, Refrigerating and Air Conditioning Engineers.

Flanders, S.N. and S.J. Marshall (1981) Interpolating R-values from thermograms. In Thermal Infrared Sensing Applied to Energy Conservation in Building Envelopes (Thermosense IV): *Proceedings of the Society of Photo-Optical Instrumentation Engineers.* Vol. 313, Bellingham, Washington.

Johannesson, G. (1979) Heat-flow measurements: thermoelectric meters, function, principles and sources of error. Lund Institute of Technology, Report TVBH-3003. Lund, Sweden (in Swedish with English summary).

Marshall, S.J. (1981) We need to know more about infrared emissivity. In Thermal Infrared Sensing Applied to Energy Conservation in Building Envelopes (Thermosense IV): *Proceedings of the Society of Photo-Optical Instrumentation Engineers.* Vol. 313, Bellingham, Washington.

Schwerdtfeger, P. (1970) The measurement of heat flow in the ground and the theory of heat flux meters. U.S.A. Cold Regions Research and Engineering Laboratory Technical Report 232.

Sonderegger, R. (1980) Accuracy limitations in determining wall U-values in the field. Draft position paper for ASTM C16.30 Task Group on Data Analysis of In-Situ Wall Thermal Performance Measurements. Berkeley, California: Lawrence Berkeley Laboratory.

Treado, S.J. (1980) Thermal resistance measurements of a built-up roof system. U.S. National Bureau of Standards, NBSIR 80-2100, Washington, D.C.

APPENDIX A. DERIVATION OF EQUATION 1

There are two avenues toward understanding the justification for eq 1, one intuitive and the other mathematical. First, we will consider the intuitive point of view.

R-value is actually defined only for steady-state conditions for temperature and heat flux:

$$R = \Delta T/Q \tag{A1}$$

where ΔT is the difference in temperature between the warm and cool sides of the test specimen and Q is the heat flow measured coming through the specimen. This simply states that every unit of temperature drop across the construction causes a proportionate measure of heat flow through it, reflecting a constant property of the constituent materials. This concept remains true for the sum of all time-varying ΔT's across a construction when compared with the sum of all time-varying Q's passing through it, both taken over a long period. The shorter the period of time, the more approximate the relationship (eq 1) because of heat temporarily stored within the construction.

Mathematical understanding of eq 1 may be obtained by paraphrasing and simplifying a derivation by Sonderegger (1980). We can characterize a construction thermally with a frequency-dependent matrix such that the temperature and heat flux on an inside surface can be described as a function of the outside temperature and flux:

$$\begin{bmatrix} \dot{T}_{in}(\omega) \\ \dot{Q}_{in}(\omega) \end{bmatrix} = \begin{bmatrix} A(\omega) & B(\omega) \\ C(\omega) & D(\omega) \end{bmatrix} \times \begin{bmatrix} \dot{T}_{out}(\omega) \\ \dot{Q}_{out}(\omega) \end{bmatrix} \tag{A2}$$

where $\dot{T}_{in}$ and $\dot{T}_{out}$ are Fourier transforms of indoor and outdoor temperatures and $\dot{Q}_{in}$ and $\dot{Q}_{out}$ are indoor and outdoor heat fluxes, respectively. $A(\omega)$, $B(\omega)$, $C(\omega)$, and $D(\omega)$ would result from matrix multiplication of each homogeneous layer represented by matrix elements of the form:

$$A(\omega) = \cosh(d^*F(\omega)) \tag{A2a}$$

$$B(\omega) = \frac{(\sinh(d^*F(\omega)))}{(k^*F(\omega))} \tag{A2b}$$

$$C(\omega) = k^*F(\omega)\sinh(d^*F(\omega)) \tag{A2c}$$

$$D(\omega) = \cosh(d^*F(\omega)) \tag{A2d}$$

$$F(\omega) = \sqrt{i\omega/\alpha} \tag{A2e}$$

where:

ω = angular frequency (rad/hr)
d = thickness of layer (m)
i = the imaginary unit
α = diffusivity of the layer (m^2/hr)
k = thermal conductivity of the layer (W/(m·k))

If we rearrange eq A2 in terms of $\dot{Q}_{in}$, we obtain:

$$\dot{Q}_{in} = (C - DA/B)\dot{T}_{out} + (D/B)\dot{T}_{in} \tag{A3}$$

which, for the purely resistive indoor air layer has values of $A = 1$, $B = d/k$ (= R-value), $C = 0$, and $D = 1$. This gives the admittances of the wall:

$$Y_1(\omega) = D(\omega)/B(\omega) \tag{A4}$$

$$Y_m(\omega) = 1/B(\omega) \tag{A5}$$

and a recharacterization of eq A3:

$$Q_{in} = Y_1(\omega)T_{in}(\omega) - Y_m(\omega)T_{out}(\omega) \tag{A6}$$

In his paper, Sonderegger treats fluctuations in diurnal outside temperatures and hourly cycling of the heating plant as sine waves. Since the effect of the heating plant cycles on the accuracy of eq 1 is negligible, it is omitted in the following discussion.

Assume that, with sinusoidal variation in outside temperature with a frequency of ω_{out}, an amplitude of A_{out}, and a phase angle at $t = 0$ of γ_{out}, we can re-express outside temperature as:

$$T_{out}(t) = \overline{T}_{out} + A_{out} * \sin(\omega_{out} * t - \gamma_{out}) \tag{A7}$$

Then, where $\overline{T}_{out}$ is the average value of $T_{out}(t)$, with a constant T_{in} and eqs A6 and A7, the indoor heat flux variation can be expressed as:

$$Q_{in}(t) = Y_1(0)T_{in} - Y_m(0)\overline{T}_{out} - |Y_m(\omega)|A_{out} * \sin(\omega_{out} * t - \gamma_{out} + \gamma_m) \tag{A8}$$

where γ_m is the phase angle of $Y_m(\omega_{out})$. For $\omega_{out} = 0$,

$$Y_1(0) = Y_m(0) = U_0 \tag{A9}$$

where U_0 is the steady-state U-value of the construction. Simplifying further, we can define $t = 0$ such that the outdoor temperature sine curve crosses zero at that time, so $\gamma_{out} = 0$. This gives

$$Q_{in}(t) = U_0 * \overline{\Delta T} - |Y_m(\omega_{out})|A_{out} * \sin(\omega_{out} * t + \gamma_m) \tag{A10}$$

where $\overline{\Delta T} = T_{in} - \overline{T}_{out}$.

Equations A7 and A10 can be rewritten as:

$$T_{in} - T_{out}(t) = \overline{\Delta T}\ [1 - (A_{out} * \sin(\omega_{out} * t))/\overline{\Delta T}\,] \tag{A11}$$

$$Q(t) = U_0 * \overline{\Delta T}\ (1 - \left(|Y_m(\omega_{out})|A_{out} * \sin(\omega_{out} * t + \gamma_m)/U_0 * \overline{\Delta T}\right) \tag{A12}$$

Now we are ready to look at the source of eq 1 by simply integrating eqs A11 and A12 and obtaining their ratio:

$$\overline{R}(t') = \frac{\int_0^{t'} (T_{in} - T_{out}(t))dt}{\int_0^{t'} (Q(t))dt} = R_0 \frac{\int_0^{t'} (1 - N)dt}{\int_0^{t'} (1 - D)dt} \tag{A13}$$

where $R_0 = 1/U_0$

$N = A_{out} * \sin(\omega_{out} * t)$

$D = |Y_m(\omega_{out})|A_{out} * \sin(\omega_{out} * t + \gamma_m)/\overline{\Delta T}$.

It is clear that N and D will always be bounded by their coefficients, whereas the rest of the integral will grow with time and dominate both numerator and denominator to approximately the ratio of one. Therefore, the longer the duration of measurement t', the more closely $\bar{R}(t')$ approximates R_0. This is the basis for demonstrating the validity of eq 1, which is simply a sum approximating eq A13.

Actual diurnal temperature cycles are not sinusoidal or even of regular amplitude. However, if one were to decompose a segment of weather history into its component cycles in a Fourier series, each component could be analyzed with eq A13. The real impact on the calculation of eq A13 from imperfect cycles would be the length of time required for N and D to become small compared with the rest of the numerator and denominator when integrated, and for $\bar{R}(t)$ to approximate R_0 satisfactorily. The steadily diminishing oscillations of $\bar{R}(t)$ about a constant value should signal when a satisfactory history of data has been obtained.

A facsimile catalog card in Library of Congress MARC format is reproduced below.

Flanders, Stephen N.
Toward in-situ building R-value measurement / by Stephen N. Flanders and Stephen J. Marshall. Hanover, N.H.: Cold Regions Research and Engineering Laboratory; Springfield, Va.: available from National Technical Information Service, 1984.
iv, 20 p., illus.; 28 cm. (CRREP Report 84-1.)
Prepared for the Office of the Chief of Engineers by U.S. Army Cold Regions Research and Engineering Laboratory under DA Project 4A762730AT42.
Bibliography: p. 8.
1. Buildings. 2. Heat flow sensors. 3. Infrared cameras. 4. Roofs. 5. R-values. 6. Thermal insulation. 7. Thermal measurement, in-situ. 8. Thermal resistance. 9. Thermocouples. 10. Thermopiles. 11. Walls.

(see CARD 2)

Flanders, Stephen N. (CARD 2)
Toward in-situ building R-value...

I. Marshall, Stephen J. II. United States. Army. Corps of Engineers. III. Cold Regions Research and Engineering Laboratory, Hanover, N.H. IV. Series: CRREL Report 84-1.

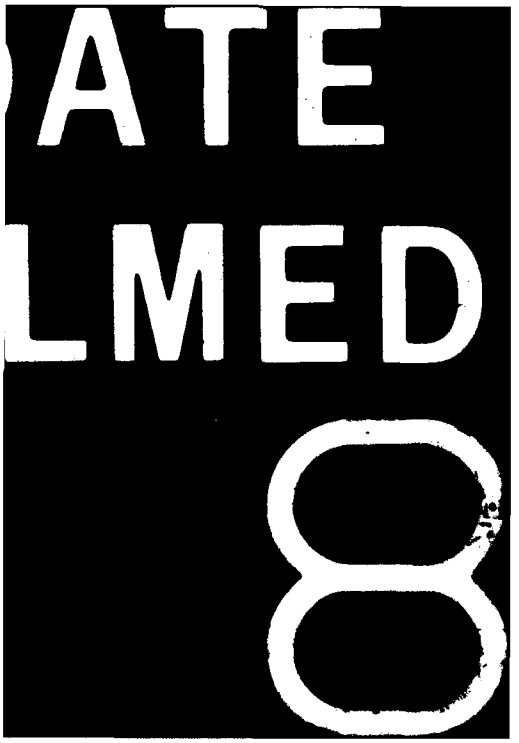
ATE
LMED
8